

Diffusion and Velocity Auto-Correlation in Shearing Granular Media

Peter Olsson

Department of Physics, Umeå University, 901 87 Umeå, Sweden

(Dated: February 4, 2022)

We perform numerical simulations to examine particle diffusion at steady shear in a model granular material in two dimensions at the jamming density and zero temperature. We confirm findings by others that the diffusion constant depends on shear rate as $D \sim \dot{\gamma}^{q_D}$ with $q_D < 1$, and set out to determine a relation between q_D and other exponents that characterize the jamming transition. We then examine the velocity auto-correlation function, note that it is governed by two processes with different time scales, and identify a new fundamental exponent, λ , that characterizes an algebraic decay of correlations with time.

PACS numbers: 45.70.-n, 64.60.-i

As the volume fraction increases in zero-temperature collections of spherical particles with repulsive contact interaction, there is a transition from a liquid to an amorphous solid state—the jamming transition. It has been suggested that this transition is a critical phenomenon with universal critical exponents [1] and the properties of this transition continues to be a very active field of research. Simulations at steady shearing have provided strong evidence that the behavior at the jamming density actually is a critical phenomenon [2, 3], but questions still remain to what extent results and ideas from ordinary critical phenomena may be taken over to the study of jamming as well as the fundamental reason for the observed critical behavior.

In critical phenomena the behavior is governed by a diverging length scale and one expects that this should also be reflected in the time dependence of various quantities. One way to probe the time dependence is to measure the particle displacements and thereby the diffusion constant. Experiments suggest that the diffusion depends algebraic on the shear rate, $D \sim \dot{\gamma}^{q_D}$, with $q_D < 1$ [4, 5]. Since this appears to be one more critical exponent, and one usually expects relations between different critical exponents, the existence of such a relation between q_D and other exponents that characterize the jamming transition is an interesting question.

In this Letter we examine the velocity auto-correlation function in an attempt to understand the behavior of the diffusion constant. A careful study of this function at very low shear rates reveals that it has both an algebraic decay and an exponential cutoff. It furthermore turns out that these two processes are governed by two different time scales, with the exponential decay being related to the externally applied time scale $\sim \dot{\gamma}^{-1}$ whereas the remaining part—which we identify with an internal relaxation—is governed by a time scale $\sim \sigma^{-1}$.

Following O'Hern *et al.* [6] we simulate frictionless soft disks in two dimensions using a Bi-dispersive mixture with equal numbers of disks with two different radii of ratio 1.4. Length is measured in units of the small particles ($d_s = 1$). With r_{ij} for the distance between the

centers of two particles and d_{ij} the sum of their radii, the interaction between overlapping particles is

$$V(r_{ij}) = \begin{cases} \frac{\epsilon}{2}(1 - r_{ij}/d_{ij})^2, & r_{ij} < d_{ij}, \\ 0, & r_{ij} \geq d_{ij}. \end{cases}$$

We use Lees-Edwards boundary conditions [7] to introduce a time-dependent shear strain $\gamma = t\dot{\gamma}$. With periodic boundary conditions on the coordinates x_i and y_i in an $L \times L$ system, the position of particle i in a box with strain γ is defined as $\mathbf{r}_i = (x_i + \gamma y_i, y_i)$. We simulate overdamped dynamics at zero temperature with the equation of motion [8],

$$\frac{d\mathbf{r}_i}{dt} = -C \sum_j \frac{dV(\mathbf{r}_{ij})}{d\mathbf{r}_i} + y_i \dot{\gamma} \hat{x}.$$

The unit of time is $\tau_0 = d_s/C\epsilon$. We take $\epsilon = 1$ and $C = 1$. We integrate the equations of motion with the Heuns method, using a time step $\Delta t = 0.2\tau_0$. As this must be considered rather large, we have checked carefully that simulations with half that time step gives the same results to a very high accuracy. The possibility to use such large time steps is linked to the simple dynamics, zero temperature, and our low shear rates.

We study a system with many particles, $N = 65536$, at ϕ_J , since the correlation length in the system should only depend on the finite shear rate and one therefore expects a simpler behavior. We have checked that our results are not affected by finite size effects. The behavior of the shear stress at three densities at and around $\phi = 0.8428$ is shown in Fig. 1. At $\phi = 0.8428$, which is our candidate for ϕ_J , the shear stress is algebraic in the shear rate, $\sigma \sim \dot{\gamma}^{q_\sigma}$ with $q_\sigma = 0.386$, whereas the data away from ϕ_J have clear curvatures. In the notation of Ref. [2], $q_\sigma = \Delta/(\beta + \Delta)$. We remark that the fit is not entirely perfect, in spite of the nice algebraic behavior in Fig. 1. This is the reason why the present estimate $\phi_J = 0.8428$ is somewhat higher than the estimate in Ref. [2]. Our new data (which extends down to lower shear rates) also show that a high-precision determination of ϕ_J and the related exponents is a difficult task. This is due to some corrections to the

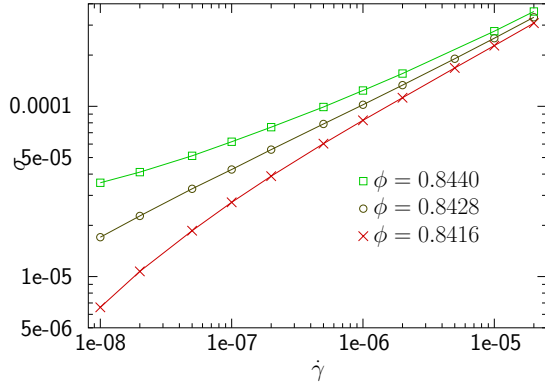


FIG. 1: Behavior at ϕ_J . At $\phi = 0.8428$ which is a good candidate for ϕ_J the shear stress depends algebraically on $\dot{\gamma}$ to a very good approximation, $\sigma \sim \dot{\gamma}^{q_\sigma}$, with $q_\sigma = 0.386$. Data at higher (squares) and lower (crosses) densities show clear curvatures.

expected scaling behavior, as will be discussed elsewhere. For the purpose of the present Letter the approximate value $\phi_J \approx 0.8428$ is, however, entirely sufficient.

We determine the diffusion constant from the transverse displacements, i.e. the displacements in the y direction, and the velocity auto-correlation function from the y component of the velocity,

$$g_v(t) = \langle v_y(t')v_y(t' + t) \rangle,$$

where the average is over all particles and a large number of initial times, t' . Here and in the following, t is the difference between two absolute times. The velocity auto-correlation function has been examined before [9], but the present data with higher precision at lower shear rates makes it possible to do a more thorough analysis of its properties. The relation to the diffusion constant is given by the fundamental relation

$$D = \int_{-\infty}^{\infty} dt g_v(t) = g_v(0) \int_{-\infty}^{\infty} dt G_v(t), \quad (1)$$

where we introduce the normalized $G_v(t) = g_v(t)/g_v(0)$. It is convenient to write the expression in terms of $G_v(t)$ both since it is the quantity that will be examined below and since the prefactor, $g_v(0)$, has a known behavior, $g_v(0) \equiv v_y^2 \sim \sigma \dot{\gamma} \sim \dot{\gamma}^{1+q_\sigma}$, which follows from $N \langle v^2 \rangle / C = L^2 \sigma \dot{\gamma}$ [9].

Some quantities related to the particle displacements are shown in Figs. 2. To make it easier to interpret the figures these quantities are plotted against γ (the strain increment), though we discuss the behavior in terms of t . Panel (a) which shows $\langle \Delta y^2 \rangle$ against γ , illustrates the crossover from ballistic motion at short times to diffusion, $\langle \Delta y^2 \rangle \sim t$. The probability distribution function (PDF) of Δy (normalized by the width of the distribution), for several different strain increments, is shown in

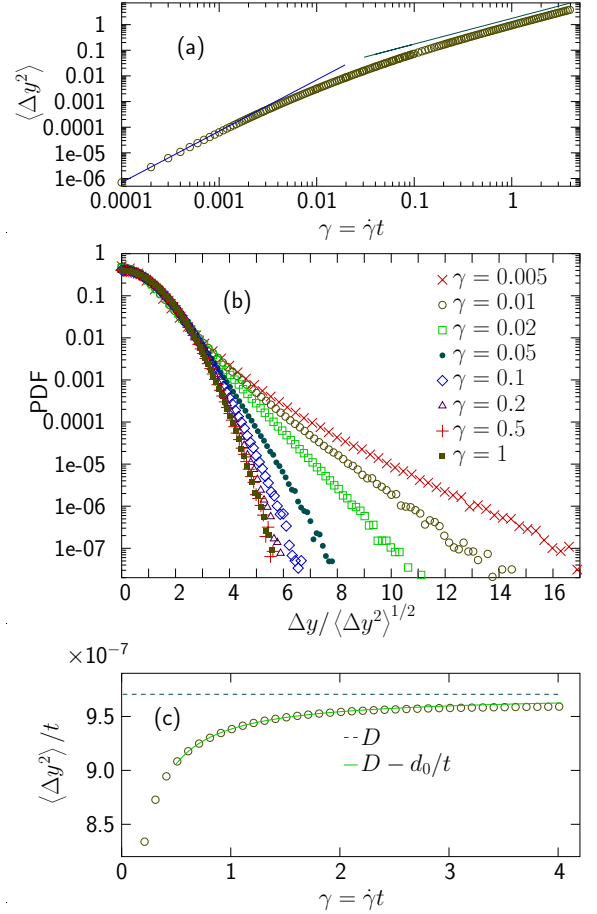


FIG. 2: Particle displacements for $\dot{\gamma} = 10^{-6}$. Panel (a) shows the crossing over of $\langle \Delta y^2 \rangle$ from ballistic behavior at short times to diffusion at large times. The slopes of the solid lines are 2 and 1, respectively. Panel (b) shows the probability distribution function of particle displacements, normalized by the width of the respective distributions. Note the exponential shape at small strains (= short times) that crosses over to a Gaussian distribution at $\gamma \approx 0.2$. Panel (c) shows the determination of D from the large γ part of the same data. The solid line is from fitting $\langle \Delta y^2 \rangle$ to Eq. (2); the dashed line corresponds to D .

panel (b). The PDF crosses over from exponential behavior at short times (small γ) to a Gaussian at longer times, as found by others [5, 10]. Our determination of the diffusion constant is illustrated in Fig. 2(c). As the figure shows it is difficult to determine D from the long time limit of $\langle \Delta y^2 \rangle / t$ since this quantity approaches the constant value $= D$ very slowly. The reason for this is a remainder of the short time behavior. For $t > t_0$, where t_0 is the range of the velocity correlations (such that $G_v(t)$ may be neglected for $t \geq t_0$; we choose $\gamma_0 = 0.5$, $t_0 = \gamma_0 / \dot{\gamma}$), it is easy to show that the expression for the mean square distance is

$$\langle \Delta y^2(t) \rangle = \int_0^t dt' \int_0^t dt'' g_v(t' - t'') = Dt - d_0 \quad (2)$$

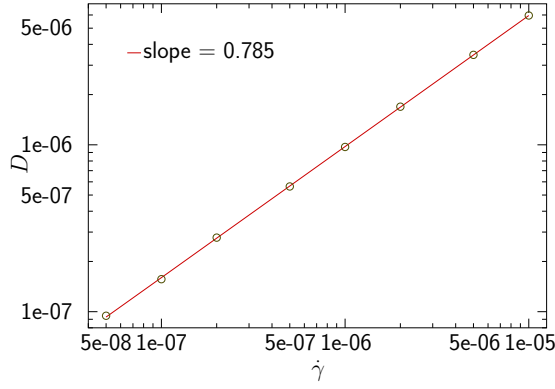


FIG. 3: Diffusion constant versus shear rate. The open circles are the diffusion constant at $\phi = 0.8428$ versus $\dot{\gamma}$. The data is well fitted to an algebraic relation $D \sim \dot{\gamma}^{q_D}$, with $q_D = 0.785(5)$.

with D from Eq. (1) and $d_0 = \int_0^{t_0} dt' \int_{t'}^{t_0} dt'' g_v(t'')$. The solid line in Fig. 2(b) is from a fit to Eq. (2) with data from the interval $\gamma_0 = 0.5 \leq \gamma \leq 2$. The dashed line is the estimated value of D .

Figure 3 shows diffusion constant versus shear rate, determined with the same kind of fits. The behavior is $D \sim \dot{\gamma}^{q_D}$, with $q_D = 0.785(5)$. This implies that the distance moved per unit strain *decreases* with increasing shear rate [11]. The corresponding exponents from experiments are $q_D = 0.80 \pm 0.01$ from three dimensional colloids [4] and $q_D = 0.66 \pm 0.05$ from bubble rafts [5]. We note that the experiments on the colloids were performed at a density close to the jamming density whereas the bubble raft was studied well above ϕ_J . This is a possible reason why the value of q_D in the colloids agrees well with our value obtained at ϕ_J .

To examine this behavior we turn to the velocity auto-correlation function which is shown in Fig. 4(a) for a range of shear rates. The same data is shown also in panel (b), but now plotted against $\gamma(t) = t\dot{\gamma}$ with a linear scale on the x axis. From this figure it seems that $\log G_v$ at large γ behaves linearly with similar slopes for different $\dot{\gamma}$, which suggests an exponential decay, $\sim e^{-\gamma(t)/\gamma_1}$. We take this to suggest that $G_v(t, \dot{\gamma})$ may be written

$$G_v(t, \dot{\gamma}) = G_v^{\text{int}}(t, \dot{\gamma}) e^{-t\dot{\gamma}/\gamma_1}, \quad (3)$$

which means that G_v is a product of an exponential decay governed by the externally imposed time scale $t_1 = \gamma_1/\dot{\gamma}$ and a function G_v^{int} , which captures the internal relaxational dynamics.

In the attempt to make sense of this data we found that a certain choice of γ_1 in Eq. (3) leads to a great simplification. It turns out that $G_v^{\text{int}}(t, \dot{\gamma})$ is then a function of the combination $t\dot{\gamma}^\kappa$,

$$G_v^{\text{int}}(t, \dot{\gamma}) = \tilde{G}(t\dot{\gamma}^\kappa),$$

and, furthermore, that this function at large values of its argument behaves algebraically, $\tilde{G}(x) \sim x^{-\lambda}$, see

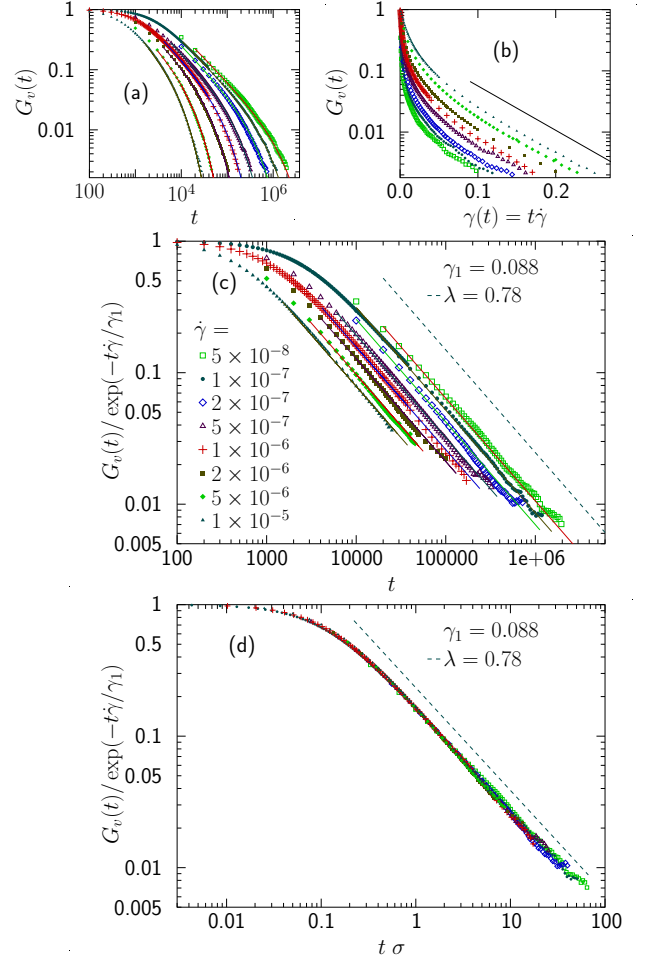


FIG. 4: The velocity auto-correlation function. Panel (a) shows the normalized auto-correlation function versus time and panel (b) is the same data against strain $\gamma(t)$. The key to our further analysis is the rectilinear behavior at large γ in panel (b) which suggests an exponential decay at large γ , $\sim e^{-\gamma(t)/\gamma_1}$. The line corresponds to $\gamma_1 = 0.06$. Panel (c) is the same data but now compensated for such an exponential decay with $\gamma_1 = 0.088$ (from fitting to Eq. (4)). Panel (d) shows the collapse, now with $t\sigma$ as the scaling variable. The scaling function obeys $\tilde{G}(x) \sim x^{-\lambda}$ for large values of its argument.

Fig. 4(c). This defines a new fundamental exponent that characterizes the relaxation dynamics, $\sim t^{-\lambda}$, though—for the accessible shear rates—it is to some extent masked by the exponential decay. To get unbiased values for these parameters, we fitted all data in the range $0.002 < G_v(t, \dot{\gamma}) < 0.3$ to

$$G_v(t, \dot{\gamma}) = A (t\dot{\gamma}^\kappa)^{-\lambda} e^{-t\dot{\gamma}/\gamma_1}, \quad (4)$$

with A , γ_1 , λ , and κ as free parameters. We find $\gamma_1 = 0.088$, $\lambda = 0.78$, and $\kappa = 0.384$. The solid lines in Fig. 4(c) show $A(t\dot{\gamma}^\kappa)^{-\lambda}$ for different $\dot{\gamma}$.

In this expression, $\dot{\gamma}^{-\kappa}$ assumes the role of a characteristic time for the internal relaxation. The observation

that $C\sigma$ has the dimension of inverse time together with the good numerical agreement between $\kappa = 0.384$ and $q_\sigma = 0.386$ (recall that $\sigma \sim \dot{\gamma}^{q_\sigma}$) suggests that $\dot{\gamma}^\kappa$ can be substituted with σ such that the scaling function may be written $\tilde{G}(t\sigma)$. Panel (d) shows the collapse when plotting against the scaling variable $t\sigma$. Note that γ_1 is the only adjustable parameter in this plot.

We now like to determine the relation between q_D and the exponents q_σ and λ that characterize the scaling of $G_v(t, \dot{\gamma})$. In the first approximation we neglect the saturation of G_v at small t , and, in effect, assume that Eq. (4) holds down to $t = 0$. This gives

$$D \sim \dot{\gamma}^{1+q_\sigma} \dot{\gamma}^{-\kappa\lambda} \left(\frac{\dot{\gamma}}{\gamma_1} \right)^{\lambda-1} \int_0^\infty dx x^{-\lambda} e^{-x} \sim \dot{\gamma}^{q_\sigma+\lambda-\kappa\lambda},$$

which leads to $q_D^{(1)} \equiv q_\sigma + \lambda - \kappa\lambda = \lambda + (1-\lambda)q_\sigma = 0.865$. This is the expected behavior as $\dot{\gamma} \rightarrow 0$, but since it is derived from a simplified $G_v(t, \dot{\gamma})$ and the result is well above $q_D = 0.785$ from Fig. 3, we next try to take the saturation of $G_v(t, \dot{\gamma})$ at small t into account and write

$$G_v(t, \dot{\gamma}) = \begin{cases} 1, & t\dot{\gamma}^\kappa < \xi_0, \\ A(t\dot{\gamma}^\kappa)^{-\lambda} e^{-t\dot{\gamma}/\gamma_1}, & t\dot{\gamma}^\kappa > \xi_0. \end{cases}$$

Assuming that $e^{-t\dot{\gamma}/\gamma_1} \approx 1$ at $t = \xi_0/\dot{\gamma}^\kappa$ (which holds to a good approximation up to our highest shear rate, $\dot{\gamma} = 10^{-5}$) the function is continuous at ξ_0 if $A = \xi_0^\lambda$. We then get

$$D = A_1 \dot{\gamma}^{q_D^{(1)}} - A_2 \dot{\gamma}, \quad (5)$$

with $A_1 = 0.235$ and $A_2 = 0.480$. As shown in Fig. 5 this expression (open circles) approaches $D \sim \dot{\gamma}^{q_D^{(1)}}$ (solid line) at small $\dot{\gamma}$ whereas there is an appreciable difference with a smaller slope at larger $\dot{\gamma}$. The diffusion constant from Fig. 3 is shown as solid dots. Note that it agrees well with the open circles from Eq. (5). It therefore seems that the measured exponent $q_D = 0.785$ is not the true asymptotic behavior.

A central conclusion from our analysis is that the full $G_v(t, \dot{\gamma})$ is approaching an algebraic behavior $\sim t^{-\lambda}$ as $\dot{\gamma} \rightarrow 0$. We now speculate that the algebraic behavior is related to the finding from quasistatic simulations that individual plastic events often are avalanches of elementary flips [12–15]. The reason for making this connection is ideas from self-organized criticality—with the paradigmatic sandpile model—that a driven system can automatically adjust itself such that there are avalanches on all length and time scales, which would be seen through power laws. With a sufficiently low shear rate (say $\dot{\gamma} = 10^{-10}$ or 10^{-9}) there would be time for the avalanches to occur one at a time and evolve according to their own dynamics. At higher shear rates other effects appear that kill off the avalanches. One possible mechanism is that a new avalanche interferes with an

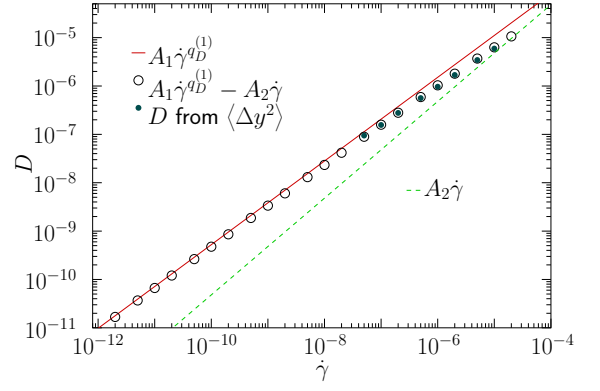


FIG. 5: Behavior of the diffusion constant. In the limit of low shear rate we expect the behavior which is given by the solid line, $D = A_1 \dot{\gamma}^{q_D^{(1)}}$. The open circles include the corrections to this behavior as given by Eq. (5). Note the good agreement with the measured D from Fig. 3. We conclude that $q_D \approx 0.785$ from the solid symbols (cf. Fig. 3), is only an effective exponent that describes the behavior in a limited range of shear rates.

existing one and thereby destroys its internal dynamics. Another possibility is that it is simply the shearing of the simulation box that destroys the correlations.

To conclude, we have found that the velocity auto-correlation function is governed by two different time scales. With $t_1 = \gamma_1/\dot{\gamma}$ from the externally applied shear rate and $t_{\text{int}} = \sigma^{-1} \sim \dot{\gamma}^{-q_\sigma}$ for the internal relaxation, the velocity auto-correlation function is $G_v(t, \dot{\gamma}) = \tilde{G}(t/t_{\text{int}}) e^{-t/t_1}$, where $\tilde{G}(x) \sim x^{-\lambda}$ for large x and λ is a new fundamental exponent. This also leads to the desired expression for q_D in terms of two fundamental exponents, $q_D = \lambda + (1-\lambda)q_\sigma$. We speculate that this algebraic decay is related to avalanches of elementary flips, and could be a manifestation of self-organized criticality.

I thank P. Minnhagen and S. Teitel for helpful discussions. This work was supported by the Swedish Research Council and the High Performance Computer Center North.

-
- [1] A. J. Liu and S. R. Nagel, *Nature (London)* **396**, 21 (1998).
 - [2] P. Olsson and S. Teitel, *Phys. Rev. Lett.* **99**, 178001 (2007).
 - [3] T. Hatano, *J. Phys. Soc. Japan* **77**, 132002 (2008).
 - [4] R. Besseling, E. R. Weeks, A. B. Schofield, and W. C. K. Poon, *Phys. Rev. Lett.* **99**, 028301 (2007).
 - [5] M. E. Möbius, G. Katgert, and M. van Hecke (2009), arXiv:0810.4211.
 - [6] C. S. O'Hern, L. E. Silbert, A. J. Liu, and S. R. Nagel, *Phys. Rev. E* **68**, 011306 (2003).
 - [7] D. J. Evans and G. P. Morriss, *Statistical Mechanics of NonEquilibrium Liquids* (Academic Press, London, 1990).

- [8] D. J. Durian, Phys. Rev. Lett. **75**, 4780 (1995).
- [9] I. K. Ono, S. Tewari, S. A. Langer, and A. J. Liu, Phys. Rev. E **67**, 061503 (2003).
- [10] P. Chaudhuri, L. Berthier, and W. Kob, Phys. Rev. Lett. **99**, 060604 (2007).
- [11] D. L. Malandro and D. J. Lacks, Phys. Rev. Lett. **81**, 5576 (1998).
- [12] C. E. Maloney and A. Lemaître, Phys. Rev. E **74**, 016118 (2006).
- [13] A. Lemaître and C. Caroli, Phys. Rev. Lett. **103**, 065501 (2009).
- [14] J. Goyon, A. Colin, G. Ovarlez, A. Ajdari, and L. Bocquet, Nature **454**, 84 (2008).
- [15] E. Lerner and I. Procaccia, Phys. Rev. E **79**, 066109 (2009).